Molecular and Cellular Biomedical Sciences, Vol.10 No.1, March 2026, p. 1-70
Print ISSN: 2527-4384, Online ISSN: 2527-3442
DOI: 10.21705/mcbs.v10n1.745

RESEARCH ARTICLE

MCBS
Mol Cell Biomed Sci. 2026; 10(1): 32-41
DOI: 10.21705/mcbs.v10n1.745

Hypoxia-Derived Mesenchymal Stem Cell Exosomes Downregulate CXCL12 and Upregulate IL-10 Expression in a Murine Model of Androgenic Alopecia

Denawati[1], Eko Setiawan[1,2], Sri Priyantini[1,3]

[1]*Department of Postgraduate Biomedical Science, Faculty of Medicine, Universitas Islam Sultan Agung, Semarang, Indonesia*
[2]*Department of Surgery, Faculty of Medicine, Universitas Islam Sultan Agung, Semarang, Indonesia*
[3]*Department of Pediatric, Faculty of Medicine Sultan Agung Islamic University, Semarang, Indonesia*

Background: Androgenic alopecia (AGA) is characterized by hair follicle miniaturization and chronic inflammation mediated by dihydrotestosterone (DHT). Current therapies primarily target hormonal pathways and do not adequately address inflammatory dysregulation. Exosomes derived from hypoxia-conditioned mesenchymal stem cells (EH-MSCs) exhibit enhanced immunomodulatory properties. However, their effects on key inflammatory mediators in AGA remain unclear. This study evaluated the effects of EH-MSCs on CXCL12 and IL-10 expression in a DHT-induced AGA mouse model.

Materials and methods: Male C57BL/6 mice were allocated into five groups: healthy control, DHT-induced alopecia without treatment, DHT-induced alopecia treated with topical minoxidil, and EH-MSCs administered at 100 or 200 µL/kgBW. Alopecia was induced by subcutaneous DHT injection for 17 days. Following model validation, treatments were administered on days 25 and 32. CXCL12 and IL-10 expression in dorsal skin tissue was analyzed using RT-PCR on day 39.

Results: DHT induction significantly increased CXCL12 expression and reduced IL-10 levels ($p<0.05$). EH-MSC administration dose-dependently downregulated CXCL12 (1.73±0.57 and 1.54±0.44 fold-change) and upregulated IL-10 expression (3.10±0.75 and 3.29±0.67 fold-change), demonstrating greater immunomodulatory effects compared with minoxidil.

Conclusion: EH-MSCs effectively modulated inflammatory biomarkers by suppressing CXCL12 and enhancing IL-10 expression in a DHT-induced AGA model, suggesting their potential as an immunoregenerative therapeutic strategy for androgenic alopecia.

Keywords: *androgenic alopecia, mesenchymal stem cells, exosomes, hypoxia, CXCL12, IL-10*

Submission: September 3, 2025
Last Revision: December 20, 2025
Accepted for Publication: January 2, 2026

Corresponding Author:
Eko Setiawan
Department of Surgery, Faculty of Medicine
Universitas Islam Sultan Agung
Terboyo Kulon, Semarang 50112, Indonesia
e-mail: drekosetiawan@unissula.ac.id

Introduction

Alopecia is a common condition affecting both men and women worldwide, with androgenic alopecia being the most prevalent subtype. Androgenetic alopecia affects up to 50% of men by the age of 50 and approximately 40% of women over 70 years, with reported prevalence rates of 30–40% in Asian men and 10–20% in Asian women.[1,2] AGA is characterized by progressive hair follicle miniaturization driven by genetic predisposition and androgen sensitivity, particularly to DHT. Beyond cosmetic concerns, AGA can significantly impair quality of life and contribute to psychological distress.[3,4]

Beyond its cosmetic implications, alopecia can significantly impair quality of life, leading to reduced self-esteem, social anxiety, and psychological distress.[5,6] Conventional therapies such as minoxidil and finasteride have shown efficacy in promoting hair regrowth. However, they are limited by side effects, variable responsiveness, and recurrence upon discontinuation.[7,8] These limitations highlight the need for regenerative medicine-based therapeutic approaches that combine efficacy and safety. Such strategies, including the use of mesenchymal stem cells (MSCs) and their secretome or exosomes, have emerged as promising modalities for tissue repair and hair follicle regeneration.

Recent advances in regenerative medicine have introduced exosomes derived from MSCs as promising candidates for tissue repair and immunomodulation.[9,10] Previous studies have demonstrated that exosomes derived from dermal papilla cells or umbilical cord MSCs stimulate hair follicle proliferation and activate proliferative signaling pathways, including RAS/ERK.[15,16] MSC-derived exosomes also enhance tissue repair by upregulating growth factors such as fibroblast growth factor-1 (FGF-1) and stromal cell-derived factor-1 (SDF-1), thereby accelerating wound healing.[17] As key mediators of hair follicle morphogenesis and regeneration, FGF-1 and SDF-1 suggest that similar regenerative pathways may underlie the therapeutic potential of exosomes in androgenetic alopecia. In addition, MSCs and their secretome exert immunomodulatory effects by suppressing pro-inflammatory cytokines and increasing interleukin-10 (IL-10) production, which is essential for follicular immune homeostasis.[11,12,18]

Consistently, exosomes from various cell sources have been shown to promote hair growth and follicular regeneration, with dermal papilla cell–derived exosomes activating β-catenin signaling and enhancing the proliferation of dermal papilla and outer root sheath cells.[19] Similarly, adipose-derived stem cell (ADSC) exosomes accelerate hair growth by upregulating the Wnt/β-catenin pathway and promoting perifollicular angiogenesis.[20] However, most studies utilized exosomes obtained under normoxic conditions, despite evidence that hypoxia enhances the regenerative and anti-inflammatory potency of MSC-derived exosomes. To date, no study has examined the effects of EH-MSCs on CXCL12 and IL-10 expression in androgenetic alopecia. This study aims to address this gap by investigating the effects of EH-MSCs on CXCL12 and IL-10 expression in an in vivo DHT-induced androgenic alopecia model using C57BL/6 mice. By examining both a pro-inflammatory chemokine (CXCL12) and an anti-inflammatory cytokine (IL-10). The findings may contribute to the development of novel exosome-based therapies that address not only follicular regeneration but also the inflammatory mechanisms underlying alopecia.

Materials and methods

Experimental Design

This study employed an experimental in vivo design, defined as an experimental approach that involves random allocation of subjects into control and treatment groups, manipulation of the independent variable (DHT induction and exosome treatment), and observation of the dependent variables (CXCL12 and IL-10 expression) after the intervention. This randomized post-test-only control group design allows for the determination of a cause-and-effect relationship between the treatment and the observed biological outcomes. All procedures carried out in this study complied with the ethical approval outlined in the ethical statement subsection.

MSCs Isolation, Hypoxic Conditioning, and Exosome Isolation

Umbilical cords were collected aseptically from 21-day pregnant C57BL/6 mice and washed with phosphate-buffered saline (PBS) (Cat. No. D8537, Merck KGaA, Darmstadt, Germany) to remove blood and debris. The Wharton's jelly was separated, minced, and cultured in Dulbecco's Modified Eagle Medium–low glucose (DMEM-LG) (Cat. No. 11885-084, Gibco™, Thermo Fisher

Print ISSN: 2527-4384, Online ISSN: 2527-3442
DOI: 10.21705/mcbs.v10n1.745

Scientific, Massachusetts, USA) supplemented with 10% fetal bovine serum (FBS) (Cat. No. 10270-106, Gibco™, Thermo Fisher Scientific, Massachusetts, USA) and 1% penicillin–streptomycin (Cat. No. 15140-122, Gibco™, Massachusetts, USA). Cells were incubated at 37 °C with 5% CO_2 and 21% O_2 under normoxic conditions.

Morphological characteristics of cultured MSCs were observed using an inverted microscope (Olympus CKX53, Tokyo, Japan) to confirm adherence and fibroblast-like spindle morphology. For immunophenotyping, cells were detached using Accutase (Cat. No. AT104, Innovative Cell Technologies, San Diego, CA, USA), washed with PBS, and resuspended at 1×10^6 cells/mL. Cells were stained with fluorochrome-conjugated antibodies against CD29 (PE; Cat. No. 303006, BioLegend, California, USA), CD90 (FITC; Cat. No. 328108, BioLegend, California, USA), CD31 (PE-Cy7; Cat. No. 303118, BioLegend, California, USA), and CD45 (APC; Cat. No. 368510, BioLegend, California, USA) for 30 minutes in the dark at room temperature. Labeled cells were analyzed using a BD FACSCanto II flow cytometer (Becton Dickinson, USA) and data were processed with FlowJo software (Tree Star, Ashland, OR, USA). For differentiation assays, MSCs at passage 3–5 were seeded at 2×10^4 cells/cm² and cultured in induction media for 21 days. Osteogenic differentiation was induced using StemPro™ Osteogenesis Differentiation Kit (Cat. No. A1007201, Thermo Fisher Scientific, Massachusetts, USA), followed by staining with Alizarin Red S (Cat. No. A5533, Sigma-Aldrich, Missouri, USA) to detect calcium deposition. Chondrogenic differentiation was induced using StemPro™ Chondrogenesis Differentiation Kit (Cat. No. A1007101, Thermo Fisher Scientific, Massachusetts, USA) and visualized with Alcian Blue 8GX staining (Cat. No. A3157, Sigma-Aldrich, Missouri, USA) to confirm proteoglycan formation.

For hypoxic preconditioning, cultures were transferred into a modular hypoxia chamber (Cat. No. 27310, Stemcell Technologies, Vancouver, Canada) maintained at 5% O_2, 5% CO_2, and 90% N_2 for 24 hours. The conditioned medium was collected and processed using tangential flow filtration (TFF; Cat. No. CEXS100A01, Repligen, Waltham, MA, USA) to obtain exosomes. The exosome protein concentration was determined by bicinchoninic acid (BCA) assay (Cat. No. 23225, Thermo Fisher Scientific, Massachusetts, USA), yielding an average of 80 µg/mL.

Exosome Characterization

Isolated exosomes were characterized using flow cytometry (BD FACSCanto II, Becton Dickinson, USA) for the surface markers CD9 and CD63 (Cat. Nos. 312102 and 353018, respectively, BioLegend, San Diego, CA, USA). Due to equipment limitations, particle size and morphology analysis (TEM/NTA) and negative marker (calnexin) evaluation were not performed. However, the use of tangential flow filtration (TFF; 100 kDa molecular weight cut-off) ensured the isolation of nanosized vesicles within the exosomal range, and the presence of specific markers CD9 and CD63 was consistent with exosomal identity.

Animal Model and Treatment Protocol

Healthy male C57BL/6 mice aged 6-8 weeks with a body weight ranging from 18-25 g were used. The animals were acclimatized for one week before experimentation and maintained under controlled laboratory conditions with ad libitum access to food and water. Sample size was calculated using Federer's formula, yielding at least five mice per group. To anticipate possible mortality, one additional animal was included in each group, resulting in six mice per group and a total of 34 mice, including those allocated for validation.

Androgenetic alopecia was induced by daily subcutaneous administration of DHT (Sigma-Aldrich, Cat. No. D073, USA) at a dose of 0.1 mg/mouse for 17 days. The development of alopecia was documented photographically every three days and confirmed microscopically using hematoxylin–eosin (H&E; Cat. No. HHS16, Sigma-Aldrich, Missouri, USA) staining.

After validation, the animals were randomly allocated into five experimental groups (n = 6 per group). Hair shaving was performed on all groups as a technical control. A healthy control group receiving no DHT or therapeutic intervention (G1); a DHT-induced alopecia group serving as an untreated positive control (G2); a DHT-induced alopecia group treated with topical 2% minoxidil (Kirkland™, USA) (G3); and two DHT-induced alopecia groups treated with intraperitoneal injections of EH-MSCs at doses of 100 µL/kg body weight (G4) and 200 µL/kg body weight (G5).

Exosome injections were given twice at one-week intervals (days 25 and 32), while minoxidil was applied topically once daily throughout the treatment period. The intraperitoneal route was selected for EH-MSC exosome administration to ensure optimal systemic absorption and bioavailability of nanosized vesicles, enabling their

paracrine and immunomodulatory effects on target tissues, including hair follicles. In contrast, minoxidil was applied topically as the standard treatment for androgenetic alopecia to exert local vasodilatory effects on the scalp. The use of different routes of administration therefore reflects the distinct pharmacological mechanisms of each treatment, local action for minoxidil versus systemic paracrine signalling for exosomes.

Tissue Harvesting and RNA Isolation

On day 39, all animals were euthanized using ketamine (80 mg/kg) and xylazine (10 mg/kg) intraperitoneally. Dorsal skin tissues were harvested aseptically, immersed in RNAlater (Invitrogen™, Waltham, MA; Cat. No. AM7020), and stored at −80°C. Total RNA was extracted using TRIzol™ reagent (Cat. No. 15596026, Invitrogen™, California, USA), and purity was verified using a NanoDrop™ 2000 spectrophotometer (Thermo Scientific, USA).

Quantitative Real-Time PCR (qRT-PCR)

Complementary DNA (cDNA) synthesis was performed using the SuperScript™ IV First-Strand Synthesis System (Cat. No. 18091050, Thermo Fisher Scientific, Massachusetts, USA). qRT-PCR was conducted using a Bio-Rad CFX96 Real-Time PCR Detection System with the following primers (Table 1). Relative gene expression was calculated using the ΔΔCt method, with GAPDH as the housekeeping gene.

Statistical Analysis

Statistical analyses were performed using SPSS software. Data were tested for normality and homogeneity before analysis. One-way ANOVA was used to compare expression levels among groups, followed by post hoc least significant difference (LSD) and Tamhane tests where appropriate. Differences were considered statistically significant at $p< 0.05$.

Results

Validation of Mesenchymal Stem Cells and Exosomes

Mesenchymal stem cells (MSCs) were successfully isolated from the umbilical cords of 21-day pregnant C57BL/6 mice and cultured up to passages 3–5. Morphologically, the cultured MSCs exhibited a fibroblast-like, spindle-shaped appearance and adhered firmly to the surface of the culture flask (Figure 1A). Flow cytometric analysis confirmed the MSC phenotype, demonstrating high expression of CD29 (98.8%) and CD90 (98.7%) and low expression of hematopoietic and endothelial markers CD45 (0.36%) and CD31 (4.81%) (Figure 1B).

The multipotency of MSCs was verified through differentiation assays. Alizarin Red staining confirmed osteogenic differentiation, while Alcian Blue staining verified chondrogenic differentiation (Figure 2A and 2B). Adipogenic differentiation was not performed due to the limited number of primary MSCs and the need to preserve early-passage cells for exosome production. According to the international society for cellular therapy (ISCT) criteria, osteogenic and chondrogenic differentiation were considered sufficient to confirm MSC multipotency.

After validation, MSCs were incubated under hypoxic conditions at 5% oxygen for 24 hours using a hypoxia chamber. The conditioned medium containing the MSC secretome was then collected and processed using a tangential flow filtration system equipped with 100–500 kDa molecular weight cut-off membranes to obtain hypoxia-derived MSC exosomes (EH-MSCs). Flow cytometry analysis confirmed the positive expression of exosomal surface markers CD9 and CD63, indicating successful isolation of exosomal fractions (Figure 3). Quantification of exosomal protein using the bicinchoninic acid (BCA) assay showed a concentration of approximately 8 µg per 100 µL, equivalent to 80 µg/mL.

Although morphological and particle-size analyses (TEM and NTA) and negative marker validation (calnexin) were not performed due to equipment limitations, the combination of size-selective isolation by TFF and the presence of exosome-specific markers (CD9 and CD63) provides sufficient evidence supporting the successful isolation of hypoxia-derived MSC exosomes (EH-MSCs).

Validation of the Androgenic Alopecia Model (AGA)

The AGA model was established in C57BL/6 mice through DHT induction. Macroscopic evaluation revealed that healthy control mice exhibited dense hair coverage, whereas DHT-induced mice displayed marked hair loss and reduced hair density (Table 2). Microscopic observation further confirmed follicular miniaturization in alopecia mice compared with healthy controls (Figure 4). These findings validated the successful induction of the androgenic alopecia model.

Print ISSN: 2527-4384, Online ISSN: 2527-3442
DOI: 10.21705/mcbs.v10n1.745

Table 1. Primer sequences used for quantitative real-time PCR analysis.

Gene	Forward Primer (5′-3′)	Reverse Primer (3′-5′)
CXCL12	ATGCCCATGCCGATTCTT	AGAGCTGCAGGGTCAAGG
IL-10	GCTCTTACTGACTGGCATGAG	CGCAGCTCTAGGAGCATGTG
GAPDH	GAAGGTGAAGGTCGAGTC	GAAGATGGTGATGGGATTTC

Modulation of CXCL12 Expression Following DHT Induction and Treatment

Analysis of CXCL12 expression demonstrated significant variations among the experimental groups (Table 3). The DHT-induced alopecia group (G2) exhibited the highest CXCL12 expression (3.15±0.53-fold relative to the control), whereas the healthy control group (G1) showed the lowest expression levels (1.00±0.35-fold). Treatment with minoxidil (G3) reduced CXCL12 expression to 2.17±0.68-fold, while administration of EH-MSC EH-MSCs were administered at doses of 100 µL/kgBW and 200 µL/kgBW, corresponding to exosomes containing approximately 8 µg and 16 µg of total exosomal protein further suppressed expression to 1.73±0.57-fold and 1.54± 0.44-fold, respectively (Figure 5).

Normality testing using the Shapiro–Wilk test confirmed that all groups had normally distributed data (p>0.05), and homogeneity was verified with Levene's test (p>0.05). One-way ANOVA analysis revealed a statistically significant difference across the groups (p<0.05). Post hoc LSD testing indicated that CXCL12 expression in the DHT group (G2) was significantly higher compared with all other groups, while treatment groups (G3–G5) showed progressively reduced expression levels compared with G2 (Table 3). The graphical representation (Figure 6) illustrated a clear downward trend in CXCL12 expression following therapeutic intervention, with the lowest values observed in the EH-MSC 200 µl group.

Upregulation of IL-10 Expression Following Treatment

IL-10 expression also varied significantly between groups (Table 4). The highest IL-10 levels were observed in the EH-MSC 200 µl group (G5) at 3.29±0.67 fold-change, followed by the EH-MSC 100 µl group (G4) at 3.10±0.75 fold-change, and the minoxidil group (G3) at 1.74±0.39 fold-change. The healthy control group (G1) demonstrated baseline levels (1.01±0.16 fold-change), while the DHT-induced alopecia group (G2) exhibited the lowest concentration (0.74±0.28 fold-change).

Normality testing using the Shapiro–Wilk test indicated normally distributed data (p>0.05). However, the Levene's test showed non-homogeneous variances across groups (p<0.05). Therefore, intergroup comparisons were conducted using Tamhane's post hoc test. Results demonstrated that IL-10 expression in the treatment groups (G3, G4, and G5) was significantly higher than in both G1 and G2. Graphical analysis confirmed a marked increase in IL-10 expression in the treated groups, with the highest upregulation observed in the EH-MSC 200 µl group.

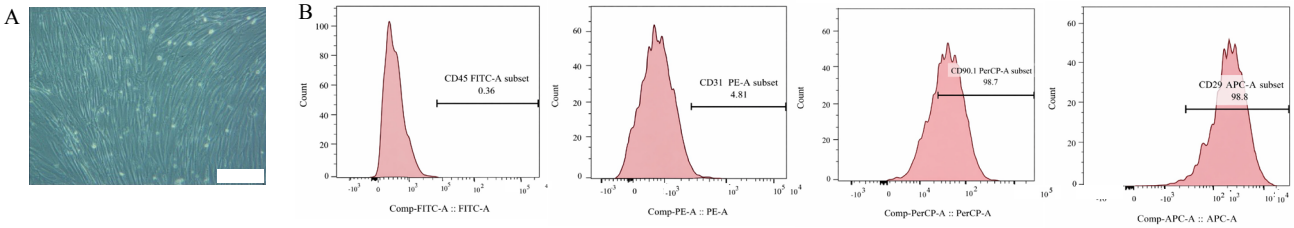

Figure 1. Morphology and Immunophenotype of MSCs. A: Morphological appearance of MSCs showing fibroblast-like, spindle-shaped cells adhering to the culture surface. B: Flow cytometry analysis of MSC surface markers showing high expression of CD29 (98.8%) and CD90 (98.7%), and low expression of hematopoietic and endothelial markers CD45 (0.36%) and CD31 (4.81%), confirming the MSC phenotype. Scale bar: 50 µm.

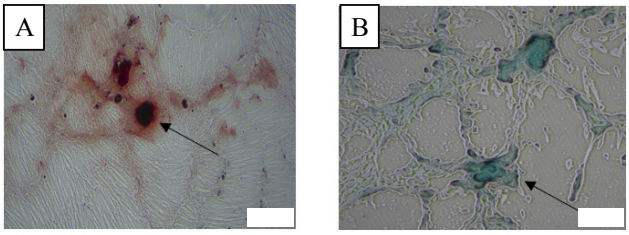

Figure 2. Morphology and immunophenotype of MSCs. A: Morphological appearance of MSCs showing fibroblast-like, spindle-shaped cells adhering to the culture surface. B: Flow cytometry analysis of MSC surface markers showing high expression of CD29 (98.8%) and CD90 (98.7%), and low expression of hematopoietic and endothelial markers CD45 (0.36%) and CD31 (4.81%), confirming the MSC phenotype. Scale bar: 50 µm.

Discussion

Validation of the alopecia model indicated that DHT induction reproduced key morphological features of human AGA, including visible hair thinning and follicular miniaturization, as observed through macroscopic and histological assessment (Table 2 and Figures 4). These changes are consistent with previous reports that DHT binds to androgen receptors in dermal papilla cells, leading to shortened anagen phases and follicular regression.[21] The macroscopic and microscopic findings in this study align with those models and establish a reliable basis for therapeutic intervention testing.

The present study demonstrated that EH-MSCs modulated key inflammatory biomarkers in a murine model of DHT-induced androgenic alopecia. The most notable findings were the downregulation of CXCL12 and the upregulation of IL-10, particularly at higher EH-MSC doses (Figures 5 and 6). These results suggest that hypoxic conditioning may enhance the immunomodulatory properties of MSC-derived exosomes, indicating their potential as a supportive approach in AGA management. The findings emphasize the dual immunoregulatory mechanism of EH-MSCs, simultaneously suppressing pro-inflammatory and enhancing anti-inflammatory mediators rather than implying therapeutic superiority over existing treatments.

One of the key findings was the significant suppression of CXCL12 expression in the EH-MSC treatment groups compared with the DHT-induced group.[22] Elevated CXCL12 in the alopecia control group is in accordance with the chemokine's known role in promoting inflammatory cell migration and sustaining a pro-inflammatory follicular microenvironment.[22–24] The reduction of CXCL12 following EH-MSC administration suggests that these exosomes modulate local inflammation, potentially preventing the recruitment of immune cells that contribute to follicular damage. Previous studies have reported that MSC exosomes attenuate CXCL12-driven inflammation in cardiovascular and autoimmune models, which corroborates the present findings.[21] This immunomodulatory effect is likely mediated by the transfer of microRNAs and proteins enriched under

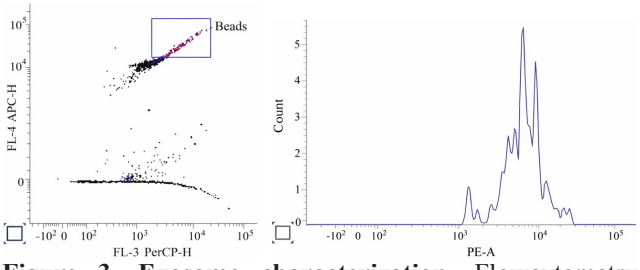

Figure 3. Exosome characterization. Flowcytometry analysis confirming the expression of exosomal surface markers CD9 and CD63 in hypoxia-derived MSC exosomes (EH-MSCs).

Table 2. Macroscopic validation of the androgenetic alopecia model and treatment response.

	After Acclimatization	One week after shaving (baseline observation)	Day 30	Day 39
G1				
G2				
G3				
G4				
G5				

Print ISSN: 2527-4384, Online ISSN: 2527-3442
DOI: 10.21705/mcbs.v10n1.745

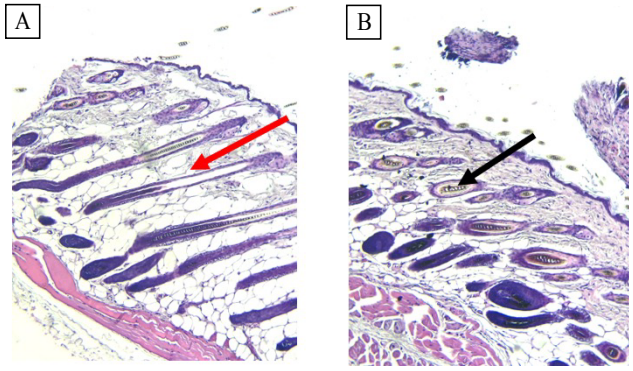

Figure 4. Microscopic validation of follicular morphology in androgenic alopecia (H&E staining). A: Healthy control group: the red arrow indicates normal hair follicles in the anagen phase, showing intact bulb structure, organized follicular orientation, and dense dermal papilla cells. B: DHT-induced AGA group: the black arrow indicates miniaturized hair follicles with reduced bulb diameter and disrupted follicular alignment, consistent with

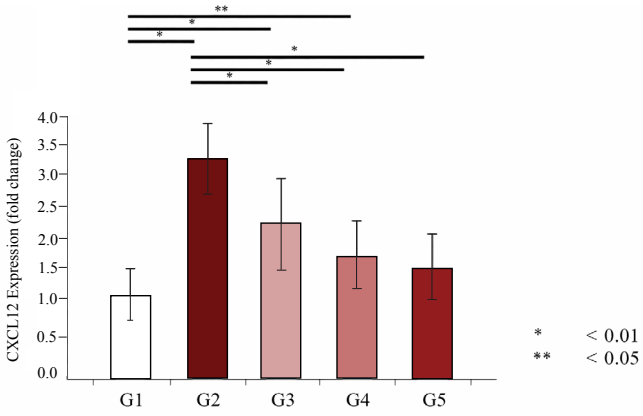

Figure 5. Pairwise comparison of fold CXCL12 expression between groups using post hoc LSD test.

hypoxic conditions, further highlighting the advantages of exosomes derived from hypoxia-preconditioned MSCs.[24,25]

The second major finding was the marked increase in IL-10 expression after EH-MSC treatment. IL-10 is a pivotal anti-inflammatory cytokine that helps maintain hair follicle immune privilege and prevents autoimmune-mediated follicular damage14. The restoration and even upregulation of IL-10 in treated groups compared with both healthy and DHT-induced controls indicate that EH-MSCs not only counteract the inflammatory state but may also enhance the protective immunological milieu around hair follicles. Importantly, hypoxia has been shown to upregulate IL-10 through hypoxia-inducible factor (HIF)-1α–dependent pathways, which may explain the superior results observed in EH-MSCs compared with normoxic exosomes.[13,25] Consistent with our findings, hypoxia-induced MSC exosomes were reported to suppress pro-angiogenic and inflammatory signalling in UVB-induced hyperpigmentation.[26] MSC secretome has also been shown to restore immune cell balance by enhancing $CD4^+$ and $CD8^+$ T cell proliferation while modulating PD-1/PD-L1 signalling in severe inflammatory conditions.[27]

Comparison with minoxidil, the current standard therapy, highlights the different therapeutic axis explored in this study. While minoxidil primarily acts through vasodilation and prolongation of the anagen phase, EH-MSCs demonstrated dual immunomodulatory activity, characterized by downregulation of CXCL12 and upregulation of IL-10.[28,29] It should be noted, however, that this study did not include a normoxic MSC exosome control group, and therefore claims of superiority cannot be made. Instead, these results underscore the potential of EH-MSCs as a novel immunomodulatory approach that targets inflammatory imbalance contributing to AGA pathology.

Table 3. CXCL12 expression analysis data.

Variable	Group					
	G1 (fold-change)	G2 (fold-change)	G3 (fold-change)	G4 (fold-change)	G5 (fold-change)	*p*-value
CXCL12	1.05±0.35	3.15±0.53	2.17±0.68	1.73±0.57	1.54±0.44	
Shapiro Wilk	0.38	0.87	0.79	0.17	0.49	
Levene test						0.53
One Way Anova						0.00

Table 4. IL-10 expression analysis data.

Variable	Group					
	G1 (fold-change)	G2 (fold-change)	G3 (fold-change)	G4 (fold-change)	G5 (fold-change)	*p*-value
IL-10	1.01±0.16	0.74±0.28	1.74±0.39	3.10±0.75	3.29±0.67	
Shapiro Wilk	0.95	0.08	0.96	0.18	0.15	
Levene test						0.02
One Way Anova						0.00

Minoxidil primarily acts by enhancing vascularization and prolonging the anagen phase, but it does not directly address inflammatory dysregulation, which is increasingly recognized as a contributing factor in AGA. The superior outcomes with EH-MSCs suggest that therapies targeting both regenerative and immunological pathways may achieve better clinical efficacy than those acting on proliferative mechanisms alone.[30]

These findings highlight the potential of EH-MSCs as a dual-function therapy for AGA, promoting follicular regeneration while modulating immune imbalance. To our knowledge, this is the first study to simultaneously assess CXCL12 suppression and IL-10 upregulation by EH-MSCs in an AGA model.[9] By demonstrating a dose-dependent effect on these markers, this research provides mechanistic insight into how hypoxia-derived exosomes can restore a favorable follicular microenvironment.[31,32] The results also support the broader therapeutic potential of EH-MSCs for chronic inflammatory conditions beyond alopecia, aligning with recent literature emphasizing exosome-based immunomodulation in regenerative medicine.[28] Several limitations should be considered when interpreting these findings. The use of a single animal model with a small sample size limits generalizability to clinical settings. Additionally, the focus on CXCL12 and IL-10 expression overlooks the complex molecular pathways involved in androgenic alopecia. The lack of long-term evaluation prevents assessment of the durability and safety of hypoxia-derived MSC exosome therapy. Future studies should use larger, diverse models, extend follow-up to evaluate sustained effects and safety, and apply multi-omics to explore broader mechanisms. Ultimately, well-designed clinical trials are necessary to confirm the translational potential of EH-MSCs for treating androgenic alopecia.

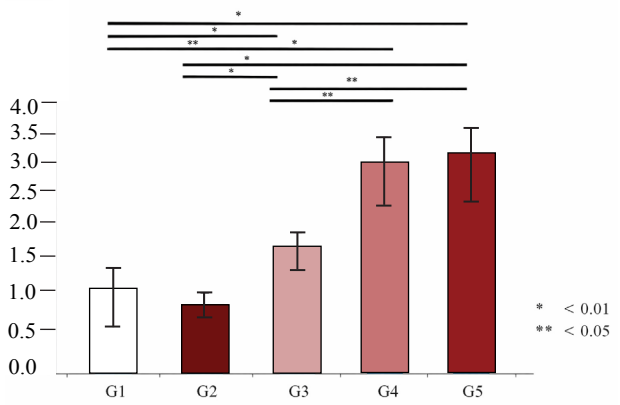

Figure 6. Pairwise comparison of fold IL-10 expression between groups using post hoc LSD test.

Conclusion

Hypoxia-derived mesenchymal stem cell exosomes significantly downregulated CXCL12 and upregulated IL-10 expression in a DHT-induced murine model of androgenic alopecia. These findings suggest that EH-MSCs modulate inflammatory pathways and may contribute to a more favorable follicular microenvironment that supports tissue regeneration. Compared with minoxidil, EH-MSCs exhibited distinct immunomodulatory effects, highlighting their potential as an alternative immunoregenerative approach for androgenic alopecia.

Authors' Contributions

DN contributed to the conceptualization and design of the study, data collection, and manuscript drafting. ES was responsible for data analysis, interpretation of results, and critical revision of the manuscript. SP provided supervision, methodological guidance, and final approval of the version to be submitted. All authors have read and approved the final manuscript.

Print ISSN: 2527-4384, Online ISSN: 2527-3442
DOI: 10.21705/mcbs.v10n1.745

Ethical Statement

The study was approved by the Bioethics Committee, Faculty of Medicine, Sultan Agung Islamic University (UNISSULA), with approval number 428/VIII/2025/ Komisi Bioetik.

Conflict of Interest

The authors declare no potential conflicts of interest with respect to the research, authorship, and/or publication of this article.

References

1. Amin SS, Sachdeva S. Alopecia areata : an update. 2013; 23(2): 209–20.
2. Lolli F, Pallotti F, Rossi A, Fortuna MC, Caro G, Lenzi A, *et al*. Androgenetic alopecia : a review. Endocrine. 2017; 57: 9-17. doi: 10.1007/s12020-017-1280-y.
3. Ghimire RB. Impact on quality of life in patients who came with androgenetic alopecia for hair transplantion surgery in a clinic rupak bishwokarma ghimire. J Nepal Med Assoc. 2018; 56(212): 763–5.
4. Dileep V, Veldi K, Chellaboina K, Metta AK, Goel A, Sai S, *et al*. Impact of androgenic alopecia on quality of life using the dermatology life quality index (DLQI): a cross-sectional study in a tertiary care hospital. Front Health Inform. 2024; 13(8): 345-54.
5. Adamowicz R, Załęcki P, Dukiel A, Nowicka D. Association between androgenetic alopecia and psychosocial disease burden: a cross-sectional survey among polish men. Dermatol Res Pract. 2022; 2022: 1845044. doi: 10.1155/2022/1845044.
6. Aukerman EL, Jafferany M. The psychological consequences of androgenetic alopecia: A systematic review. J Cosmet Dermatol. 2023; 22(1): 89–95.
7. Martora F, Vastarella M, Fattore D, Patri A, Fabbrocini G, Cantelli M. Oral minoxidil for chemotherapy-induced alopecia. Ski Appendage Disord. 2022; 8(6): 508–10.
8. Suchonwanit P, Thammarucha S, Leerunyakul K. Minoxidil and its use in hair disorders: A review. Drug Des Devel Ther. 2019; 13: 2777–86.
9. Pan Q, Wang Y, Lan Q, Wu W, Li Z, Ma X, et al. Exosomes derived from mesenchymal stem cells ameliorate hypoxia/reoxygenation-injured ECs via transferring MicroRNA-126. Stem Cells Int. 2019; 2019(1): 2831756. doi: 10.1155/2019/2831756.
10. Liang Y, Tang X, Zhang X, Cao C, Yu M, Wan M. Adipose mesenchymal stromal cell-derived exosomes carrying MiR-122-5p Antagonize the inhibitory effect of dihydrotestosterone on hair follicles by targeting the TGF-β1/SMAD3 signaling pathway. Int J Mol Sci. 2023; 24(6): 5703. doi: 10.3390/ijms24065703.
11. Zheng M, Kim MH, Park SG, Kim WS, Oh SH, Sung JH. CXCL12 Neutralizing Antibody Promotes Hair Growth in Androgenic Alopecia and Alopecia Areata. Int J Mol Sci. 2024; 25(3): 1705. doi: 10.3390/ijms25031705.
12. Wojciechowska-Zdrojowy M, Jankowska-Konsur A, Nowicka-Suszko D, Szepietowski JC, Hryncewicz-Gwóźdź A. Comparison of serum concentrations of interleukins 10, 12, 17 and 35 between patients with alopecia areata and controls. Postep Dermatologii i Alergol. 2021; 38(6): 1052–7.
13. Wang G, Wang Z, Zhang J, Shen Y, Hou X, Su L, *et al*. Treatment of androgenetic alopecia by exosomes secreted from hair papilla cells and the intervention effect of LTF. J Cosmet Dermatol. 2023; 22(11): 2996–3007.
14. Li Y, Wang G, Wang Q, Zhang Y, Cui L, Huang X. Exosomes Secreted from adipose-derived stem cells are a potential treatment agent for immune-mediated alopecia. J Immunol Res. 2022; 2022(1): 7471246. doi: 10.1155/2022/7471246.
15. Mao Y, Liu P, Wei J, Xie Y, Zheng Q, Hu X, *et al*. Exosomes derived from umbilical cord mesenchymal stem cell promote hair regrowth in C57BL6 mice through upregulation of the RAS/ERK signaling pathway. J Transl Intern Med. 2024; 12(5): 478–94.
16. Ntshingila S, Oputu O, Arowolo AT, Khumalo NP. Androgenetic alopecia: An update. JAAD Int. 2023; 13: 150–8.
17. Hariani NP, Putra A, Subchan P, Setiawan E. Mesenchymal stem cell-derived exosomes enhance FGF-1 and SDF-1 expression in rats with second degree burns. Mol Cell Biomed Sci. 2025; 9(2): 115-23.
18. Widowati W, Faried A, Kusuma HSW, Hermanto Y, Harsono AB, Djuwantono T. Allogeneic mesenchymal stem cells and its conditioned medium as a potential adjuvant therapy for COVID-19. Mol Cell Biomed Sci. 2023; 7(1):1-9.
19. Li J, Zhao B, Dai Y, Zhang X, Chen Y, Wu X. Exosomes derived from dermal papilla cells mediate hair follicle stem cell proliferation through the Wnt3a / β -Catenin signaling pathway. 2022; 2022(1): 9042345. doi: 10.1155/2022/9042345.
20. Zhou Y, Seo J, Tu S, Nanmo A, Kageyama T, Fukuda J. Exosomes for hair growth and regeneration. J Biosci Bioeng. 2024; 137(1): 1-8.
21. Watson VE, Faniel ML, Kamili NA, Krueger LD, Zhu C. Immune-mediated alopecias and their mechanobiological aspects. Cells Dev. 2022; 170: 203793. doi: 10.1016/j.cdev.2022.203793.
22. Qin J, Shang L, Ping AS, Li J, Li X jun, Yu H, *et al*. TNF/TNFR signal transduction pathway-mediated anti-apoptosis and anti-inflammatory effects of sodium ferulate on IL-1β-induced rat osteoarthritis chondrocytes in vitro. Arthritis Res Ther. 2012; 14(6): R242. doi: 10.1186/ar4085.
23. Li K, Sun Y, Liu S, Zhou Y, Qu Q, Wang G, *et al*. The AR/miR-221/IGF-1 pathway mediates the pathogenesis of androgenetic alopecia. Int J Biol Sci. 2023; 19(11): 3307–23.
24. Kang K, Ma R, Cai W, Huang W, Paul C, Liang J, *et al*. Exosomes secreted from CXCR4 overexpressing mesenchymal stem cells promote cardioprotection via Akt signaling pathway following myocardial infarction. Stem Cells Int. 2015; 2015(1): 659890. doi: 10.1155/2015/659890.
25. Zhang X, Bao P, Zheng Q, Chu M, Liang C, Guo X, *et al*. Comparative Analysis of mRNA and miRNA Expression between Dermal Papilla Cells and Hair Matrix Cells of Hair Follicles in Yak. Cells. 2022; 11(24): 3985. doi: 10.3390/cells11243985.
26. Andavania SJ, Syamsunarno MR, Putra A, Setiawan E. Hypoxia-induced mesenchymal stem cell exosomes modulate protein kinase A and VEGFR expression in ultraviolet b-induced hyperpigmentation in mice. Mol Cell Biomed Sci. 2025; 9(2): 91-7.
27. Soleha W, Wibowo H, Abdullah M, Pradipta S, Syari LN, Liem IK, *et al*. UC-MSCs secretome induces proliferation of CD4+ T cells, CD8+ T cells, NK cells, and increases sPD-1 levels in severe

COVID-19's whole blood. Mol Cell Biomed Sci. 2025; 9(1): 39-47.
28. Norouzi F, Aghajani S, Vosoughi N, Sharif S, Ghahremanzadeh K, Mokhtari Z, *et al*. Exosomes derived stem cells as a modern therapeutic approach for skin rejuvenation and hair regrowth. Regen Ther. 2024; 26: 1124–37.
29. González-Cubero E, González-Fernández ML, Gutiérrez-Velasco L, Navarro-Ramírez E, Villar-Suárez V. Isolation and characterization of exosomes from adipose tissue-derived mesenchymal stem cells. J Anat. 2021; 238(5): 1203–17.
30. Zheng M, Oh SH, Choi N, Choi YJ, Kim J, Sung JH. CXCL12 inhibits hair growth through CXCR4. Biomed Pharmacother. 2022; 150(February): 112996. doi: 10.1016/j.biopha.2022.112996.
31. Anjum M, Rajasekar S, Prashant K. Mesenchymal stem cell conditioned media induces hair regeneration in alopecia areata: a case study. Ann Stem Cell Res Ther. 2021; 5(1):1041.
32. Deng W, Zhang Y, Wang W, Song A, Mukama O, Huang J, *et al*. Hair follicle-derived mesenchymal stem cells decrease alopecia areata mouse hair loss and reduce inflammation around the hair follicle. Stem Cell Res Ther. 2021; 12(1) :1–11.